Cholesterol Adsorption from Artificial Human Plasma with Molecular Imprinted Polymeric Nanostructures

Moleküler Baskılanmış Polimerik Nanoyapıları ile Yapay İnsan Plazmasından Kolesterol Adsorpsiyonu

Research Article

Tülden Inanan[1,2]* and Nalan Tüzmen[3]

[1]Dokuz Eylul University, The Graduate School of Natural and Applied Sciences, Izmir, Turkey.
[2]Aksaray University, Tech. Voc. Sch. of Higher Education, Dept. of Chem. and Chemical Processing Technology, Aksaray, Turkey.
[3]Dokuz Eylul University, Faculty of Science, Chemistry Division, Izmir, Turkey.

ABSTRACT

This study reports cholesterol adsorption from artificial human plasma using MIP nanostructures prepared with different template:monomer ratios. The adsorption capacity of CP is 19.9% and 16.1% higher than those of C3P and CP3, respectively and adsorption capacity of CP is significantly higher than NIP nanostructures. All selectivity coefficients and relative selectivity values were higher than 1 for artificial human plasma. Under optimum conditions, considerably high cholesterol was adsorbed from hypercholesterolemic plasma (95.33 %).

Key Words
Cholesterol; molecular imprinting; plasma; nanostructures.

ÖZ

Bu çalışma, farklı kalıp-monomer oranları kullanılarak hazırlanmış MIP nanoyapıları ile yapay insan plazmasından kolesterol adsorpsiyonunu sunmaktadır. CP'nin adsorpsiyon kapasitesi C3P ve CP3'e göre sırayla %19,9 ve %16,1 daha yüksektir ve CP'nin adsorpsiyon kapasitesi NIP nanoyapılarına göre önemli derecede yüksektir. Tüm seçicilik katsayıları ve bağıl seçicilik değerleri yapay insan plazması için 1'den büyüktür. Optimum koşullarda, hiperkolesterolemik plazmadan oldukça yüksek kolesterol (%95.33) adsorplanmıştır.

Anahtar Kelimeler
Kolesterol; moleküler baskılama; plazma; nanoyapılar.

INTRODUCTION

Molecular imprinted polymers (MIPs) are multi-purpose synthetic materials which are contemplated with pre-specified selectivity for a target molecule [1-4]. MIPs gain certain interest due to their selectivity to target molecules [5]. In comparison with biological counterparts such as antibodies, enzymes or biological receptors, MIPs have superior advantages: easy to prepare, good physical and chemical stability, economic, and applicability in harsh chemical media without loss of binding features [6-8].

In the preparations of MIPs, firstly functional monomers are arranged around the template and polymerized in the presence of cross-linking agent [7,9]. Covalent [10] or noncovalent interactions [11-13] can be exploited to organize the functional monomers around the template [14]. Recognition and binding properties are influenced by the functional monomers, cross-linker used in polymerization. In addition, cross-linking degree and monomer:template ratio are critical parameters for MIP performance [15-16].

This rapidly developing technique that ensured excellent molecular recognition [17] has potential use in chromatographic separations, [18], sensors [19-21] and several extraction methods [22-23]. Extraction or determination of several molecules by MIPs were applied to environmental samples such as tap, river, well, lake, surface, waste and pond water samples; to biological samples such as urine, plasma, serum, blood and to food matrices such as milk, tomato, egg [24].

Cholesterol is one of the important biological molecule that is precursor of bile acids and steroid hormones. However, high cholesterol levels in blood induce coronary heart disease, arteriosclerosis, myocardial infarction, brain thrombosis, lipid metabolism dysfunction, hypertension, etc [25]. Thus, studies by several methods including physical, chemical, and biomedical approaches [26] had been done for cholesterol removal [27]. Physical methods are based on adsorption by hybrid material [28] supercritical fluid extraction [29], hydrophobic adsorbent [30] and molecular imprinted technique [28, 31-33].

In this study, MIP nanostructures were prepared by surfactant free emulsion co-polymerization using different monomer:template ratios (1:1 [35]; 1:3 and 3:1) and applied for cholesterol adsorption from artificial human plasma. N-Methacryloylamido-(L)-phenylalanine methyl ester (MAPA) and 2-hydroxyethyl methacrylate (HEMA) were used as monomers and ethylene glycol dimethacrylate (EGDMA) and cholesterol were used as the cross-linker and the template, respectively. Pre-polymerization complexes were characterized by FTIR, UV and NMR spectroscopies. After polymerization process, 86% of imprinted cholesterol was removed and removed template was identified by high performance liquid chromatography (HPLC) and FTIR. Cholesterol adsorption onto nanostructures was studied from commercial human plasma by investigating the effects of solvent and dilution ratio. Finally, cholesterol adsorption was applied from hypercholesterolemic plasma.

MATERIALS and METHODS

Materials

HEMA (99%) was supplied from Fluka. Methacyloyl chloride, EGDMA, cholesterol and human plasma were supplied from Sigma. Poly(vinyl alcohol) (PVA, high molecular weight, more than 99%) and potassium persulphate (KPS) were purchased from Merck. All organic solvents were chromatographic- and all other chemicals were analytical-grade. Deionised water was obtained from a Millipore S.A.S 67120 Molsheim-France facility.

Preparation and Characterization of Pre-Polymerization Complexes

The synthesis of MAPA co-monomer was performed in accordance with the method of Say et al. [34]. Pre-polymerization complexes of cholesterol with MAPA were prepared with the template:monomer ratio as 1:1 [35], 1:3 and 3:1; and termed as CP, CP3 and C3P. Cholesterol solution was prepared in THF and mixed with MAPA at room temperature for 3 h in the dark. Preparation procedures of pre-polymerization complexes were summarized in Table 1.

Table 1. Preparation procedures of pre-polymerization complexes.

	CP (1:1)	CP3 (1:3)	C3P (3:1)
CHO	4.950×10^{-5} mol	4.950×10^{-5} mol	1.485×10^{-4} mol
(M_W: 386.7 g/mol-30mg/mL)	638 μL	638 μL	1914 μL
MAPA	4.950×10^{-5} mol	1.485×10^{-4} mol	4.950×10^{-5} mol
(M_W: 234 g/mol-0.34 g/mL)	34 μL	102.2 μL	34 μL

Characterization of pre-polymerization complexes was carried out with UV, NMR, and FTIR spectroscopies. Cholesterol, MAPA and pre-polymerization complexes were scanned to determine maximum wavelengths with UV-spectrophotometer (Schimadzu 1601, Japan). H-NMR spectra of MAPA and pre-polymerization complexes were taken by liquid MERCURYplus-AS 400 with 400 mHz operation frequency. FTIR spectra of cholesterol, MAPA and pre-polymerization complexes were recorded with FTIR spectrophotometer (Perkin Elmer spectrum 100 FT-IR spectrometer) with a universal ATR sampling accessory.

Preparation and Characterization of Cholesterol Imprinted and Non-Imprinted Polymeric Nanopheres

Synthesis of MIP and NIP nanostructures could be summarized as: pre-polymerization complexes were added to stabilizer solution, 0.2775 g PVA in 25 mL water, and suspended for 5 min. HEMA (600 μL) and EGDMA (300 μL) were added as functional monomer and cross-linker, respectively. Finally, KPS (0.0198 g in 45 mL distilled water) was added as the initiator and polymerization mixture was sonicated and mixed to homogenate. After N_2 flow for 5 min, polymerization was initiated at 70°C and shacked at 65 rpm for 24 h in a temperature controlled water bath shaker (GFL 1092). Non-imprinted polymeric (NIP) nanostructures were synthesized by the same method without adding cholesterol into polymerization mixture. Characterization studies such as FTIR analysis, particle size measurement, and scanning electron microscopy (SEM) analysis were performed synthesis and characterization data for MIP with the template:monomer ratio as 1:1 were given in our previous study [35].

Thermal gravimetric (TG) and derivated thermal gravimetric (DTG) curves at the thermal degradation of cholesterol imprinted and non-imprinted polymeric nanostructures were evaluated by an EXSTAR S11 7300 at a heating rate of 10°C/min.

Template Removal Studies

Various template removal solutions were studied for the determination of the most efficient one. Surfactants such as cetyl trimethylammonium bromide (CTAB), sodium dodecyl sulfate (SDS) and triton X-100 (0.00001%), $(NH_4)_2SO_4$ solution (0.1 M) and THF were tested for template removal and performed two times at room temperature by shaking at 225 rpm for 2 h. Cholesterol concentrations of template removal solutions were analyzed with HPLC. Also, template removal supernatants were concentrated under N_2 stream and were analyzed by FTIR spectrophotometer with a universal ATR sampling accessory (Perkin Elmer spectrum 100 FTIR spectrometer).

Cholesterol Adsorption Studies from Artificial Human Plasma

Firstly, adsorption capacities of MIP and NIP nanostructures were identified in methanol. 100 ppm cholesterol solution prepared in methanol was adsorbed onto 1 mg MIP and NIP nanostructures for 30 min (saturation period for adsorption) at room temperature. Polymeric nanostructures were separated by centrifugation at 12000 rpm. Initial and final cholesterol concentrations were determined by HPLC.

Artificial human plasma was used for cholesterol adsorption and different dilution ratios were tested for the determination of matrix effect and dilutions were performed with

50 mM pH 7.4 phosphate buffer and methanol to specify the most appropriate solvent. All diluted plasma solutions were used in cholesterol adsorption studies. Final solutions removed from nanostructures were filtered (0.2 μm Sartorius filter) and analyzed by HPLC. For cholesterol adsorption from hypercholesterolemic plasma, artificial human plasma was diluted with methanol at 1:5 dilution ratio. Then, it was spiked with 1000 ppm CHO solution (prepared in methanol) at 5:9 volume ratio. Initial cholesterol concentration of spiked artificial plasma for hypercholesterolemic plasma experiments was determined as 265 mg/dL. All cholesterol adsorption experiments were performed in three replicates. For each set of data, standard statistical methods were used to determine the mean values and standard deviations. Confidence intervals of 95% were calculated for each set of samples in order to determine the margin of error.

Selectivity Experiments

Selectivity experiments were performed by competitive adsorption of progesterone, testosterone, estrone and estradiol that are the analogues of CHO. Artificial human plasma was spiked with estrone, estradiol, progesterone and testosterone as all components would be at some concentration with CHO.

Cholesterol analogues were quantified by the method of group Navakova with some modification with HPLC. HPLC analyses of estron (E1), estradiol (E2), testosterone (T) and progesterone (P) were perfomed with Thermo Hypersil Gold 150x4.6mm, 5μ column and acetonitrile:methanol:1% acetic acid (40:30:30, v/v/v) as mobile phase at 1.2 mL/min at 30°C [36]. Retention times for E1, E2, T and P at 225 nm were 2.5, 2.7, 3.0 and 4.8 min, respectively. For determination of selectivity, selectivity coefficient and relative selectivity were calculated by using equations below:

$$K_d = (C_i - C_f) / C_f \times V/m = Q/C_f \qquad (1)$$

where K_d represents the distribution coefficient (mL/g); C_i and C_f are initial and final concentrations of cholesterol (mg/L), respectively. V is the sample volume (L) and m is the nanostructure weight (g).

$$k = K_d(cholesterol)/K_d(X) \qquad (2)$$

$$k' = k(MIP)/k(NIP) \qquad (3)$$

where k represents selectivity coefficient; X is the cholesterol analogue and k' is relative selectivity.

RESULTS and DISCUSSION

Characterization of Pre-Polymerization Complexes

Complexation between monomers and template molecules has been observed by changes in spectroscopic properties of the complexes. Maximum absorption wavelengths for cholesterol and MAPA were detected as 205 nm and 318 nm, respectively. All pre-polymerization complexes have UV absorption peaks at 310 nm. Shifts observed at the maximum wavelengths of pre-polymerization complexes demonstrated the complexation of cholesterol with MAPA.

FTIR spectra of pre-polymerization complexes were recorded for comparison of incorporation into pre-polymerization complexes and given in Figure 1. Stretching vibrations of O-H and C-O of cholesterol were observed at 3530 cm^{-1} and 1053 cm^{-1}, respectively. An intensive band at 1740 cm^{-1} and a band at 1020 cm^{-1} correspond to C=O and C-O stretching of MAPA, respectively. The peak observed at 750 cm^{-1} was due to aromatic character in MAPA. O-H and C-H stretching (3400 and 2900 cm^{-1}) and C-H bending (1100 cm^{-1}) vibrations of cholesterol were seen in pre-polymerization complexes. Asymmetric C=O stretching vibration (1750 cm^{-1}) of MAPA was also seen in pre-polymerization complexes. On the other hand, the intensities of N-H stretching vibrations of MAPA (3400-3500 cm^{-1}) and O-H stretching vibrations of cholesterol (3400 cm^{-1}) decreased in pre-polymerization complexes. These findings demonstrate the complexation of cholesterol with MAPA. O-H and C-H stretching and C-H bending vibrations were sharper in C3P than the others because of the higher incorporation of cholesterol into pre-polymerization complex structure. Aromatic C=C stretching vibration, seen in both cholesterol and MAPA (sharper), were detected in
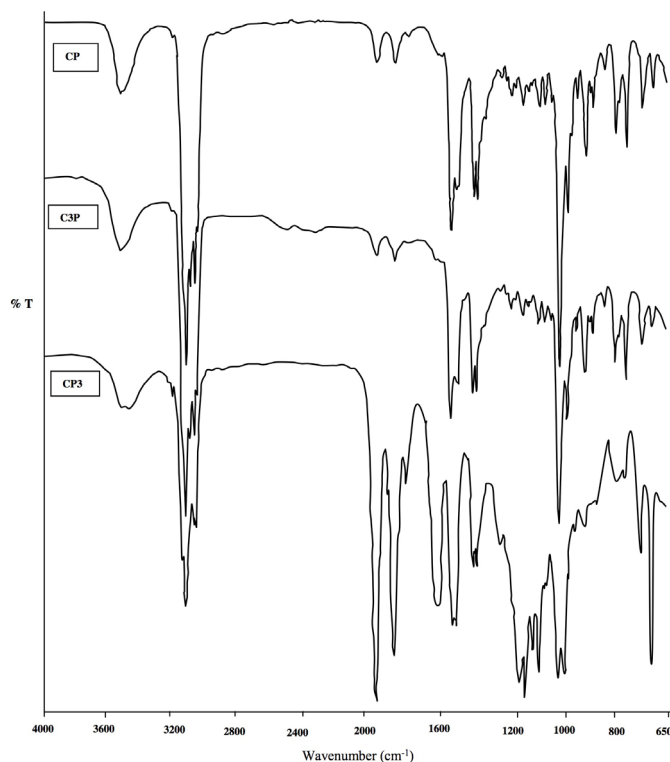
Figure 1. FTIR spectra of pre-polymerization complexes (CP, C3P, CP3).

all pre-polymerization complexes but sharper in CP3. Also, asymmetric C=O stretching vibrations are sharper in CP3 than the others. These findings can be resulted from higher incorporation of MAPA into CP3 pre-polymerization structure.

^{1}H-NMR chemical shift ranges for MAPA in $CDCl_3$ were specified as (ppm) = 1.78 (s, 3H, CH3); 5.32 (s, H, =CH_2), 5.57 (s, H, =CH_2), 5,62 (s, 1H, CH); 7.17 (d, 1H, ArH); 7.23 (d, 2H, 2xArH); 7.25 (t, 2H, 2xArH), 8.29 (s, 1H, NH)

^{1}H-NMR chemical shift ranges for CP pre-polymerization complex in $CDCl_3$ were specified as (ppm) = 0.86 (d, 6H, 2xCH_3); 0.91 (d, 3H, CH_3); 1.00 (s, 3H, CH_3); 1.07-1.22 (m, 8H, 4xCH_2), 1.25 (s, 3H, CH_3); 1.32-1.60 (m, 17H), 1.65 (d, 1H, CH), 1.92 (s, 3H, CH_3); 1.95-2.08 (m, 2H, CH_2); 2.23-2.30 (m, 2H, CH_2); 3.49-3.55 (m, 1H, CH); 3.71 (t, 1H, CH); 3.73 (d, 2H, CH_2); 5.34 (m, 1H, =CH); 7.08-7.12 (m, 2H, 2xArH); 7.23-7.31 (m, 3H, 3xArH).

Shifts (around 7 ppm) belong to aromatic CH protons of MAPA. Proton belonging to C=C of cholesterol is seen at 5.34 ppm. Shifts at 3.71 and 3.73 ppm belong to MAPA. CH proton of polar head of cholesterol is seen around 3.5 ppm. Shifts between 0-2.3 ppm belong to CH, CH_2 and CH_3 protons of cholesterol and CH_3 protons of MAPA. OH proton of cholesterol and -NH proton of MAPA are not seen in H-NMR spectrum of pre-polymerization complex. The absence of these chemical shifts makes us think that interactions between cholesterol and MAPA in pre-polymerization complex occur at these regions. Similar shifts were determined for C3P and CP3 correlatively to the ones of CP. The very few interactions for cholesterol binding are either H-bonding or hydrophobic interactions [37]. Polar chemical groups, such as -OH group in methanol do not cause the hydrophobic effect. H-bonding interactions occur in methanol. Thus, it may be concluded that interactions at cholesterol binding to imprinted nanostructures will be H-bonding. It was supposed that binding of several steroids to MIPs were mainly occurred through H-bonding interactions [38]. Consequently, possible interactions between template and functional monomer may be H-bonding.

Characterization of Cholesterol Imprinted Polymeric Nanostructures

TG and DTG curves at the thermal degradation of cholesterol imprinted and non-imprinted polymeric nanostructures were given in Figure 2. As seen in Figure 2, the temperature point for the maximum weight loss based on the curve of DTG was 367, 408, 403 and 364°C for CP (green), CP3 (black), C3P (blue) and NIP (red) nanostructures, respectively. Degradation rates of polymeric nanostructures followed the order NIP > CP3 > C3P > CP. DTG curves of all polymeric nanostructures demonstrated high thermal resistance. At about 200°C, the polymers exhibited an obvious weight loss because of the loss of water or solvent molecules captured in the polymeric nanostructures. Therefore, this temperature was the initial decomposition temperature. In the range of 300-460°C, polymeric nanosheres had two processes of weight loss, which was due to the production of co-polymers between HEMA and MAPA. The results showed that the prepared polymeric nanostructures have good thermal stability [33].

Template Removal Studies

Polymeric nanostructures were washed with methanol and water. Some of cholesterol was removed by ultrasonication effect in methanol washing. Several solutions were tested to remove the residual template from nanostructures.

Total cholesterol removal percentage was increased to 85.8% with THF [35], 70.3% with $(NH_4)_2SO_4$, 76.7% with Triton X-100, 74.7% with SDS, 75.7% with CTAB, and. Most efficient template removal was achieved by ultrasonic effect in MeOH and subsequent THF washings. Cholesterol was removed from all imprinted polymeric nanostructures and then, these nanopheres were washed with water several times to avoid from solvent remnant.

FTIR spectra of removal solution concentrated under N_2 stream (a) and cholesterol standard (b) were matched and all the bands found in standard cholesterol spectrum were determined in the spectrum of removal solution. Shifts seen at some bands and also changes at the intensities of some bands might be due to chemical changes at cholesterol structure in the synthesis of pre-polymerization complexes.

Cholesterol Adsorption Studies from Human Plasma

Adsorption capacities of all imprinted polymeric nanostructures were identified with 100 ppm standard cholesterol in methanol to
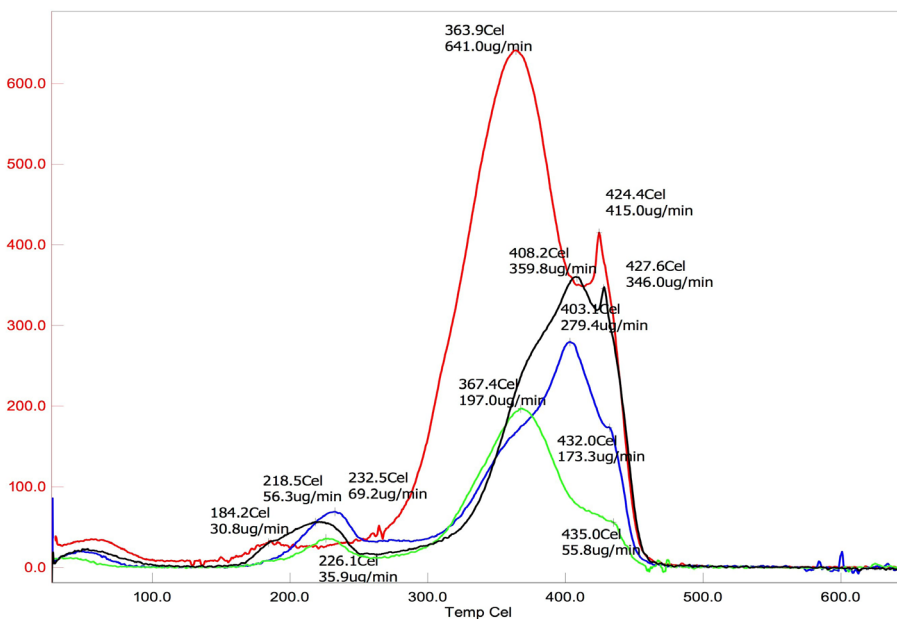

Figure 2. DTG curves of CP (green), CP3 (black), C3P (blue) and NIP (red) nanostructures.
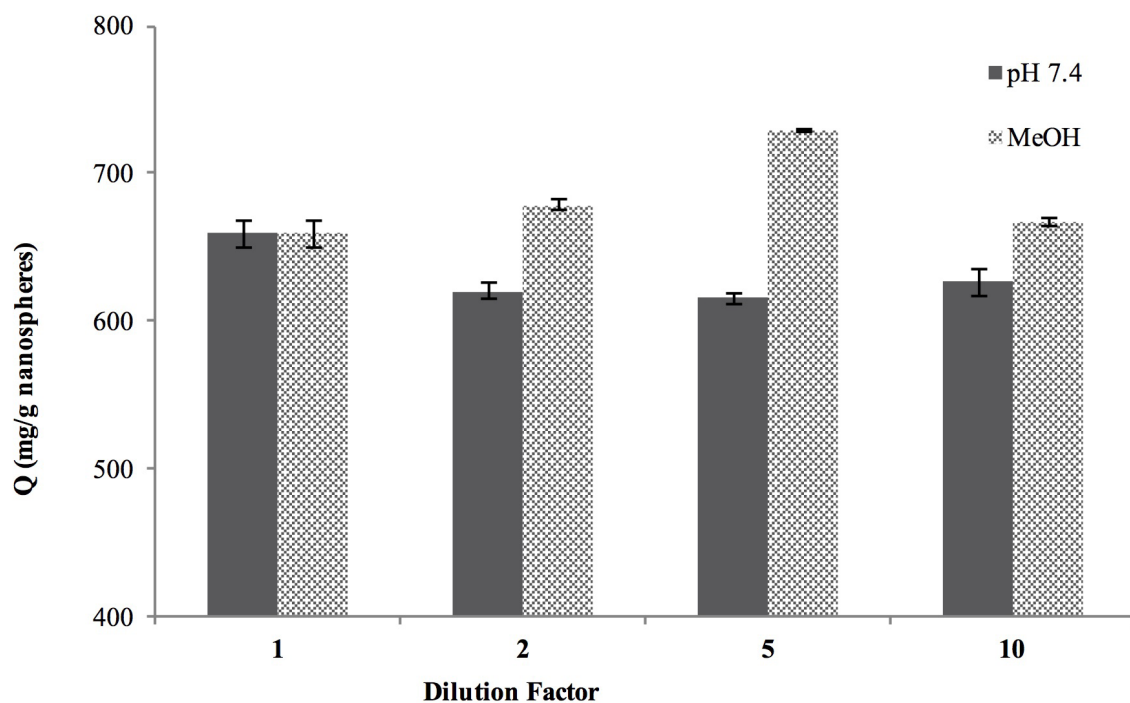
Figure 3. Adsorption capacity of CP nanostructures from artificial human plasma in different dilution solution and ratio (25°C, 225 rpm, 1 mg nanostructures).

determine the effect of monomer:template ratio. Cholesterol adsorption capacities of CP, C3P and CP3 nanostructures were determined as 25.9 [35], 21.6 and 22.3 mg/g nanostructures. The adsorption capacity of CP is 19.9% and 16.1% higher than those of C3P and CP3, respectively. Then, cholesterol adsorption studies were performed with CP nanostructures from artificial human plasma with several dilutions with the 50 mM phosphate buffer (pH 7.4) and methanol to determine the effects of dilution ratios and dilution solutions. Cholesterol adsorption capacity of CP nanostructures from artificial human plasma in different dilution solution and ratio were given in Figure 3.

As seen in Figure 3, adsorption capacity of CP nanostructures was higher with methanol dilution than the one with pH 7.4 phosphate buffer. 1:5 dilution with methanol was the most favorable one and applied in further cholesterol adsorption studies from human plasma. In this optimum conditions, cholesterol adsorption capacities of CP, C3P and CP3 nanostructures were determined and given in Figure 4.

As seen in Figure 4, cholesterol adsorption capacities were detected as 729.4, 693.9 and 715.4 mg/g for CP, C3P and CP3 nanostructures and 647.8 mg/g nanostructures for NIP, respectively. It can be concluded that CP nanostructures are more effective in cholesterol removal from human plasma. This result, compatible with the result from adsorption capacity in methanol, can be concluded that monomer:template ratio 1:1 is more convenient for cholesterol imprinting. The high adsorption capacity of NIP from artificial human plasma was a result of non-specific hydrophobic interactions.

Cholesterol removal percentage of CP nanostructures from hypercholesterolemic plasma was calculated as high as 95.33%. This result clearly shows that these CP nanostructures can be used effectively for cholesterol removal from human plasma.

Selectivity Experiments
Selectivity experiments were performed by competitive adsorption of progesterone, testosterone, estrone and estradiol that are the
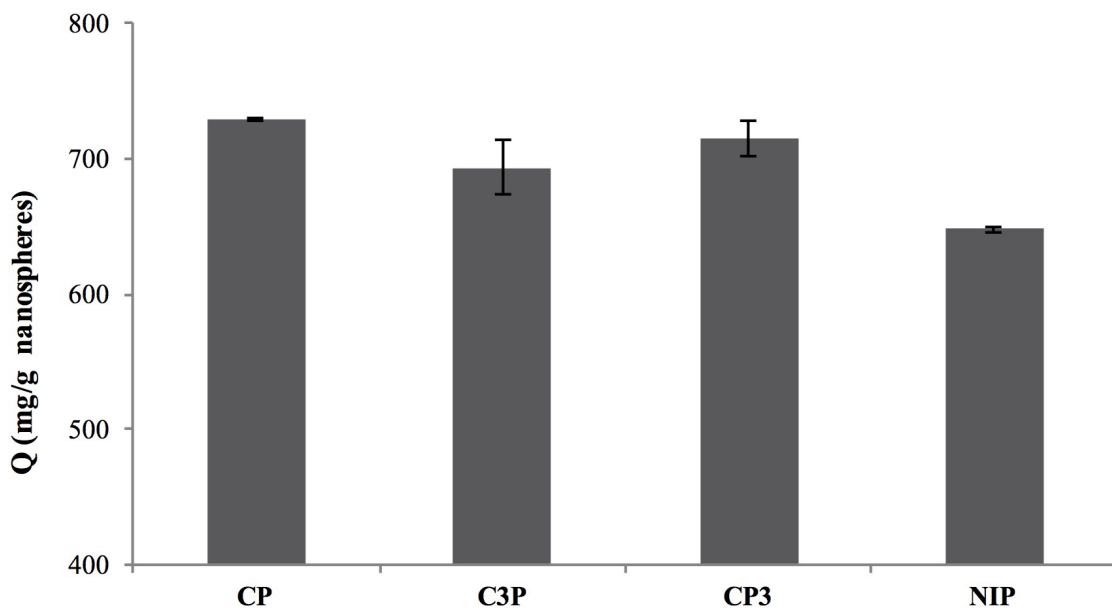
Figure 4. Cholesterol adsorption capacities of CP, C3P and CP3 nanostructures from artificial human plasma (25°C, 225 rpm, 1 mg nanostructures).
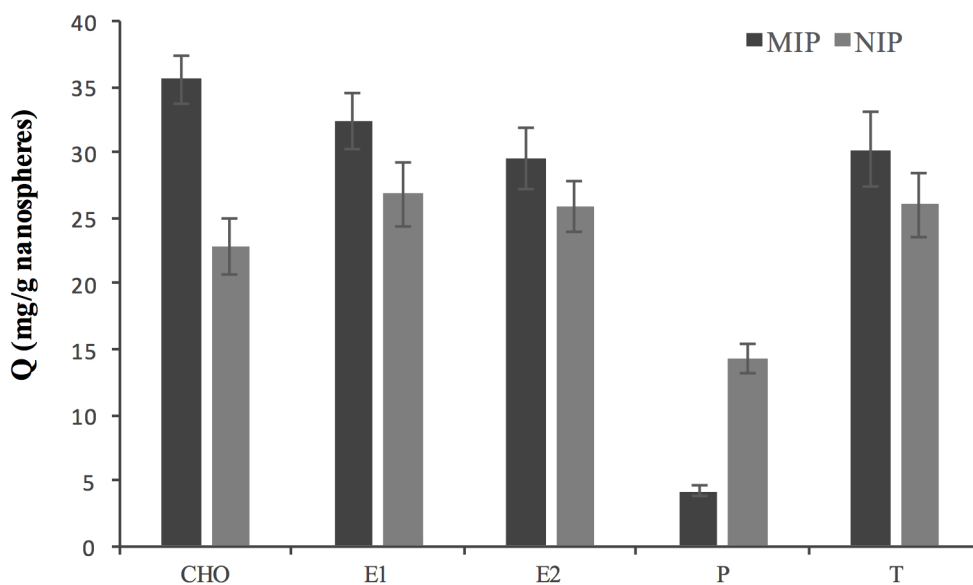

Figure 5. Amount of cholesterol and its analogues adsorbed onto MIP and NIP nanostructures in artificial human plasma (25°C, 225 rpm, 1 mg nanostructures).

Table 2. Selectivity coefficients and relative selectivities for artificial human plasma.

	$k = K_d(CHO)/K_d(x)$	$k' = k\,(MIP)/k(NIP)$
CHO-E1	1.130	1.377
CHO-E2	1.267	1.480
CHO-T	1.233	1.453
CHO-P	10.781	6.259

Table 3. Comparison of the CHO imprinted nanostructures with the reported adsorbents for cholesterol. removal.

Adsorbents	Removal % or Q (mg/g)	Medium	Ref.
Tetraethyl orthosilicate adsorption coloumn with artificial neural networks (ANN) models	67.8%	Milk	[40]
-cyclodextrin	95.9%	Milk	[41]
CHO-imprinted poly(GMA-N-methacryloyl-(L)-tyrosine microspheres embedded p(HEMA) cryogels	80% and 42.2 mg/g	Milk and IMS	[42]
Cholesterol imprinted poly(HEMA-N-methacryloyl-(L)-tyrosine methylester)	7.7 mg/g	IMS	[43]
CHO imprinted poly(HEMA-methacryloyloamidotryphan) particles embedded composite membrane	9.24 mg/g	IMS	[44]
Cholesterol imprinted poly(HEMA-N-methacryloyl-(L)- phenylalanine methylester)	11.72 mg/g	IMS	[35]
Co-precipitation, kneading, physical mixture complexation methods with -cyclodextrin	91.54; 27.85 and 16.81 %	Butter	[45]
-cyclodextrin immobilized chitosan beads cross-linked with 1,6-hexamethylene diisocyanate	92%	Egg yolk (30-fold diluted)	[46]
Thymus vulgaris L. Powder before and after milling	47 and 38%	Human serum	[47]
CHO imprinted granular polymers by co-polymerization on the surface of selenium nanoparticles	40.2%	Blood plasma	[48]
Random and oriented anti-LDL antibody immobilized p(HEMA) cryogel	111 and 129 mg LDL/g	Hypercholesterolemic plasma	[49]
Cholesterol imprinted solid-phase extraction sorbents with methacrylic acid	92.7 and 91.1% recovery	CHO std. serum and human serum	[50]
Cholesterol imprinted solid-phase extraction sorbents with methacrylic acid	80.4 and 86.6% recovery	Yolk and milk	[50]
Cholesterol imprinted solid-phase extraction sorbents with methacrylic acid	81.4 and 80.1% recovery	Pork and beef	[50]
Cholesterol imprinted poly(HEMA-N-methacryloyl-(L)- phenylalanine methylester)	729.4 mg/g	Artificial human plasma	This work
Cholesterol imprinted poly(HEMA-N-methacryloyl-(L)- phenylalanine methylester)	95.3%	Hypercholesterolemic plasma	This work

analogues of CHO. Artificial human plasma was spiked with estrone, estradiol, progesterone and testosterone as all components would be at some concentration with CHO.

Adsorption of cholesterol and its analogues was performed from plasma to determine the selectivity of MIP nanostructures. Amount of cholesterol and its analogues adsorbed onto MIP and NIP nanostructures were given in Figure 5.

As seen in Figure 5, amount of cholesterol adsorbed onto MIP nanostructures was higher than that of its analogues. For NIP nanostructures, amount of adsorbed estrone (E1), estradiol (E2) and testosterone (T) was higher than that of cholesterol. Using these results, selectivity coefficients and relative selectivity values have been calculated and given in Table 2.

All selectivity coefficients and relative selectivity values for artificial human plasma were higher than 1. These results demonstrate that adsorption of cholesterol onto MIP nanostructures was more selective than NIP nanostructures. Moreover, MIP nanostructures adsorbed cholesterol more selectively than its analogues in artificial human plasma. The relative selectivity value for CHO-P was calculated higher than those values for other analogues.

CONCLUSION

Monomer-template ratio is one of the parameters that are very effective on MIPs' performance [16,28,39]. In this study, cholesterol imprinted polymeric nanostructures were prepared by free surfactant emulsion polymerization with different monomer:template ratios. Characterization studies of pre-polymerization complexes by NMR and FTIR suggested that cholesterol may be complexed with MAPA by H-bonding interactions. Template removal was successfully performed by 85% with methanol and THF. Thermal characterizations proved that imprinted polymeric nanostructures were resistant to high temperatures such as 400°C. Dilution of plasma with methanol 5-times decreases the shielding effect of the plasma medium and increases the removal efficacy greatly. Moreover, notably high

cholesterol removal efficacy was achieved by MIP nanostructures from hypercholesterolemic plasma. Cholesterol removal efficiency of MIP nanospheres were compared with reported adsorbents and given in Table 3. Selectivity coefficients indicate that adsorption of cholesterol onto MIP nanostructures was more selective than NIP nanostructures. Relative selectivity values show that MIP nanostructures adsorbed cholesterol more selectively than its analogues in artificial human plasma.

References

1. S.N. Hashim, R.I. Boysen, L.J. Schwarz, B. Danylec, M.T. Hearn, A comparison of covalent and non-covalent imprinting strategies for the synthesis of stigmasterol imprinted polymers, J. Chromatogr. A, 1359 (2014) 35-43.
2. E. Verheyen, J.P. Schillemans, M. Wijk, M.A. Demeniex, W.E. Hennink, C.F. Nostrum, Challenges for the effective molecular imprinting of proteins, Biomaterials, 32 (2011) 3008-3020.
3. M. Behbahani, S. Bagheri, M.M. Amini, H.S. Abandansari, H.R. Moazami, A. Bagheri, Application of a magnetic molecularly imprinted polymer for the selective extraction and trace detection of lamotrigine in urine and plasma samples, J. Sep. Sci., 37 (2014) 1610-1616.
4. C. Lu, H. Li, M. Xu, S. Wang, G. Li, W. Zhong, S.Qin, Preparation of nicotine-imprinted monolith by insitu surface imprinting onto internal hole surface of macroporous silica for selective enrichment and separation of nicotine in environmental water sample, Sep. Sci. Technol., 50 (2015) 2124-2133.
5. J. Ding, F. Zhang, X. Zhang, L. Wang, C. Wang, Q. Zhao, Y. Xu, L. Ding, N. Ren, Determination of roxithromycin from human plasma samples based on magnetic surface molecularly imprinted polymers followed by liquid chromatography-tandem mass spectrometer, J. Chromatogr. B, 1021 (2016) 221-228.
6. X. Xu, S. Liang, X. Meng, M. Zhang, Y. Chen, D. Zhao, Y. Li, A molecularly imprinted polymer for the selective solid-phase extraction of dimethomorph from ginseng samples, J. Chromatogr. B, 988 (2015) 182-186.
7. X. Kong, R. Gao, X. He, L. Chen, Y. Zhang, Synthesis and characterization of the core−shell magnetic molecularly imprinted polymers (Fe_3O_4@MIPs) adsorbents for effective extraction and determination of sulfonamides in the poultry feed, J. Chromatogr. A, 1245 (2012) 8-16.
8. M. Andaç, I.Y. Galaev, A. Denizli, Affinity based and molecularly imprinted cryogels: Applications in biomacromolecule purification, J. Chromatogr. B, 1021 (2016) 69-80.

9. J. Yang, Z. Wang, T. Zhou, X. Song, Q. Liu, Y. Zhang, L. He, Determination of cyproheptadine in feeds using molecularly imprinted solid-phase extraction coupled with HPLC, J. Chromatogr. B, 990 (2015) 39-44.

10. C. Hwang, W.C. Lee, Chromatographic characteristics of cholesterol imprinted polymers prepared by covalent and non-covalent imprinting methods, J. Chromatogr. A, 962 (2002) 69-78.

11. E. Caro, N. Masque, R.M. Marce, F. Borrull, P.A.G. Cormack, D.C. Sherington, Non-covalent and semi-covalent molecularly imprinted polymers for selective on-line solid-phase extraction of 4-nitrophenol from water samples, J. Chromatog. A, 963 (2002) 169-178.

12. F. Lanza, A.J. Hall, B. Sellergen, A. Bereczki, G. Horvai, S. Bayoudh, P.A.G. Cormack, D.C. Sherington, Development of semiautomated procedure for the synthesis and evaluation of molecularly imprinted polymers applied to the search for functional polymers for phenytoin and nifedipine, Anal. Chim. Acta, 435 (2001) 91-106.

13. A. Ersöz, A. Denizli, İ. Şener, A. Atılır, S. Diltemiz, R. Say, Removal of phenolic compounds with nitrophenol-imprinted polymer based on p-p and hydrogen-bonding interactions, Sep. Purif. Technol., 38 (2004) 173-179.

14. R. Say, A. Ersöz, İ. Şener, A. Atılır, S. Diltemiz, A. Denizli, Comparison of adsorption and selectivity characteristics for 4 nitrophenol imprinted polymers prepared via bulk and suspension polymerization, Sep. Sci. Technol., 39 (2004) 3471-3484.

15. E. Yılmaz, K. Mosbach, K. Haupt, Influence of functional and cross-linking monomers and the amount of template on the performance of molecularly imprinted polymers in binding assays, Anal. Commun., 36 (1999) 167-170.

16. C.H. Hu, T.C. Chou, Albumin molecularly imprinted polymer with high template affinity-prepared by systematic optimization in mixed organic/aqueous media, Microchem. J., 91 (2009) 53-58.

17. X. Sun, J. Wang, Y. Li, J. Yang, J. Jin, S.M. Shah, J. Chen, Novel dummy molecularly imprinted polymers for matrix solid-phase dispersion extraction of eight fluoroquinolones from fish samples, J. Chromatog. A, 1359 (2014) 1-7.

18. S. Aşir, D. Sari, A. Derazshamshir, F. Yılmaz, K. Şarkaya, A. Denizli, Dopamine imprinted monolithic column for capillary electrochromatography, Electrophoresis, 0 (2017) 1-10.

19. A.G. Sarıkaya, B. Osman, T. Çam, A. Denizli, Molecularly imprinted surface plasmon resonance (SPR) sensor for uric acid determination, Sens. Actuators B Chem., 251 (2017) 763-772.

20. G. Sener, E. Ozgur, E. Yılmaz, L. Uzun, R. Say, A. Denizli, Quartz crystal microbalance based nanosensor for lysozyme detection with lysozyme imprinted nanoparticles. Biosens. Bioelectron., 26 (2010) 815-821.

21. Y. Saylan, S. Akgönüllü, D. Çimen, A. Derazshamshir, N. Bereli, F. Yılmaz, A. Denizli, Development of surface plasmon resonance sensors based on molecularly imprinted nanofilms for sensitive and selective detection of pesticides, Sens. Actuators B Chem., 241 (2017) 446-454.

22. L.I. Andersson, Molecular imprinting for drug bioanalysis A review on the application of imprinted polymers to solid-phase extraction and binding assay, J. Chromatogr. B, 739 (2000)163-173.

23. E. Turiel, A. Martin-Esteban, Molecularly imprinted polymers for sample preparation: a review, Anal. Chim. Acta, 66 (2010) 887-899.

24. L. Chen, S. Xu, X. Li, Recent advances in molecular imprinting technology: current status, challenges and highlighted applications, Chem. Soc. Rev., 40 (2011) 2922-2942.

25. A. Aghaei, M.R.M. Hosseini, M. Najafi, A novel capacitive biosensor for cholesterol assay that uses an electropolymerized molecularly imprinted polymer, Electrochimica Acta, 55 (2010) 1503-1508.

26. A. Sinha, S. Basiruddin, A. Chakraborty, N.R. Jana, Cyclodextrin functionalized magnetic mesoporous silica colloid for cholesterol separation, ACS Appl. Mater. Interfac., 7 (2015) 1340-1347.

27. Y. Su, Y. Tian, R. Yan, C. Wang, F. Niu, Y. Yang, Study on a novel process for the separation of phospholipids, triacylglycerol and cholesterol from egg yolk, J. Food Sci. Technol., 52 (2015) 4586-4592.

28. D.N. Clausen, I.M.R. Pires, C.R.T. Tarley, Improved selective cholesterol adsorption by molecularly imprinted poly(methacrylic acid)/silica ($PMAA-SiO_2$) hybrid material synthesized with different molar ratios, Mat. Sci. Eng. C, 44 (2014) 99-108.

29. M.M. Jimenez-Carmona, M.D.L. de Castro, Reverse micelle formation for acceleration of the supercritical fluid extraction of cholesterol from food samples, Anal. Chem., 70 (1998) 2100-2103.

30. E.E.G. Rojas, J.S.D. Coimbra, L.A. Minim, Adsorption of egg yolk plasma cholesterol using a hydrophobic adsorbent, Eur. Food Res. Technol., 223 (2006) 705-709.

31. A. Zengin, E. Yildirim, U. Tamer, T. Caykara, Molecularly imprinted superparamagnetic iron oxide nanoparticles for rapid enrichment and separation of cholesterol, Analyst, 138 (2013) 7238-7245.

32. Y. Tong, H. Guan, S. Wang, J. Xu, J. He, Syntheses of chitin-based imprinting polymers and their binding properties for cholesterol, Carbohyd. Res., 346 (2011) 495-500.

33. R. Gupta, A. Kumar, Synthesis and characterization of sol–gel-derived molecular imprinted polymeric materials for cholesterol recognition, J. Sol-Gel Sci. Technol., 58 (2011) 182-194.

34. R. Say, S. Emir, B. Garipcan, S. Patir, A. Denizli, Novel methacryloylamidophenylalanine functionalized porous chelating beads for adsorption of heavy metal ions, Adv. Polym. Tech., 22 (2003) 355-364.

35. T. Inanan, N. Tuzmen, S. Akgöl, A. Denizli, Selective cholesterol adsorption by molecular imprinted polymeric nanospheres and application to GIMS, Int. J. Biol. Macromolec., 92 (2016) 451-460.

36. L. Navakova, P. Solich, L. Matysova, J. Sıcha, HPLC determination of estradiol, its degradation product, and preservatives in new topical formulation estrogel HBF, Anal. Bioanal. Chem., 379 (2004) 781-787.

37. M.A. Gore, R.N. Karmalkar, M.G. Kulkarni, Enhanced capacities and selectivities for cholesterol in aqueous media by molecular imprinting: role of novel cross-linkers, J. Chromatog. A, 804 (2004) 211-221.

38. X. Li, M. Li, J. Li, F. Lei, X. Su, X. Liu, P. Li, X. Tan, Synthesis and characterization of molecularly imprinted polymers with modified rosin as a cross linker and selective SPE-HPLC detection of basic orange II in foods, Anal. Met., 6 (2014) 6397-6406.

39. H.S. Andersson, J.G. Karlsson, S.A. Piletsky, A.C. Koch-Schmidt, K. Mosbach, I.A. Nicholls, Study of the nature of recognition in molecularly imprinted polymers, influence of monomer–template ratio and sample load on retention and selectivity, J. Chromatogr. A, 848 (1999) 39-49.

40. G.R. Oliveira, A.V. Santos, A.S. Lima, C.M.F. Soares, M.S. Leite, Neural modelling in adsorption column of cholesterol-removal efficiency from milk, LWT- Food Science and Technol., 64 (2015) 632-638.

41. D.K. Lee, J. Ahn, H.S. Kwak, Cholesterol removal from homogenized milk with β-cyclodextrin, J Dairy Sci., 82 (1999) 2327-2330.

42. K. Çaktü, G. Baydemir, B. Ergün, H. Yavuz, Cholesterol removal from various samples by cholesterol-imprinted monosize microsphere-embedded cryogels, Artif. Cells Nanomed. Biotechnol., 42 (2014) 365-375.

43. H. Yavuz, V. Karakoç, D. Türkmen, R. Say, A. Denizli, Synthesis of cholesterol imprinted polymeric particles, Int. J. Biol. Macromol., 41 (2007) 8-15.

44. M. Odabaşı, L. Uzun, G. Baydemir, N.H. Aksoy, Ö. Acet, D. Erdönmez, Cholesterol imprinted composite membranes for selective cholesterolrecognition from intestinal mimicking solution, Colloids Surf. B Biointer., 163 (2018) 266–274.

45. H.M.A.M. Dias, F. Berbicz, F. Pedrochi, M.L. Baesso, G. Matioli, Butter cholesterol removal using different complexation methods with beta-cyclodextrin, and the contribution of photoacoustic spectroscopy to the evaluation of the complex, Food Res. Int., 43 (2010) 1104–1110.

46. S.H. Chiu, T.W. Chung, R. Giridhar, W.T. Wu, Immobilization of b-cyclodextrin in chitosan beads for separation of cholesterol from egg yolk, Food Res. Int., 37 (2004) 217-223.

47. E. Salehi, S. Afshar, M.Z. Mehrizi, A. Chehrei, M. Asadi, Direct reduction of blood serum cholesterol using Thymus vulgaris L.: Preliminary biosorption study, Process Bichem., accepted manuscript

48. I. Polyakova, L. Borovikova, A. Osipenko, E. Vlasova, B. Volchek, O. Pisarev, Surface molecularly imprinted organic-inorganic polymers having affinity sites for cholesterol, React. Funct. Polym., 109 (2016) 88-98.

49. N. Bereli, G. Şener, H. Yavuz, A. Denizli. Oriented immobilized anti-LDL antibody carrying poly(hydroxyethyl methacrylate) cryogel for cholesterol removal from human plasma, Mater. Sci. Eng. C, 31 (2011) 1078–1083.

50. Yun S., J.H. Zhang, D.Shi, M. Jiang, Y.X. Zhu, S.R. Mei, Y.K. Zhou, K. Dai, B. Lu, Selective solid-phase extraction of cholesterol using molecularly imprinted polymers and its application in different biological samples, J. Pharm. Biomed. Anal., 42 (2006) 549–555.